LA-UR- 10-03715

Approved for public release; distribution is unlimited.

Title: Thomson Parabola Ion Energy Analyzer

Author(s): J. A. Cobble, K. A. Flippo, S. A. Letzring, F. E. Lopez, D. T. Offermann, J. A. Oertel, D. Mastrosimone

Intended for: 40th Annual Anomalous Absorption Conference, Aspen, CO, June 13 - 18, 2010

Los Alamos
NATIONAL LABORATORY
EST. 1943

Thomson Parabola Ion Energy Analyzer

Jim Cobble, Kirk Flippo, Sam Letzring, Frank Lopez, Dustin Offerman, John Oertel
Los Alamos National Laboratory
Dino Mastrosimone, University of Rochester

A new, versatile Thomson parabola ion energy (TPIE) analyzer has been designed and constructed for use at the OMEGA-EP facility. Multi-MeV ions from EP targets are transmitted through a W pinhole into a (5- or 8-kG) magnetic field and subsequently through a parallel electric field of up to 30 kV/cm. The ion drift region may have a user-selected length of 10, 50, or 80 cm. With the highest fields, 500-MeV C^{6+} and C^{5+} may be resolved. TPIE is TIM-mounted at OMEGA-EP and is qualified in all existing TIMs. The instrument runs on pressure-interlocked 15-VDC power available in EP TIM carts. It may be inserted to within several inches of the target to attain sufficient flux for a measurement. For additional flux control, the user may select a square-aperture W pinhole of 0.004" or 0.010". The detector consists of CR-39 backed by an image plate. The fully relativistic design code and design features are discussed. Ion spectral results from first use at OMEGA-EP are expected.

Los Alamos NATIONAL LABORATORY EST. 1943

UNIVERSITY of ROCHESTER

LA-UR 09-06920

Motivation for Versatility

For the first test of a Thomson parabola on EP, flexibility was imperative. OMEGA-EP performance is improving monthly, and it was necessary to prepare for a variety of ion fluxes and ion energies. Energy resolution is important.

• On TPIE, *the flux* is controlled by

1) the input-aperture pinhole
2) the distance from the ion source.

These control the collection solid angle: the opening area and R^2.

• *The energy bandwidth* is controlled by the length of the ion drift region. The longer the drift region, the greater the ion energy dispersion – more cm/MeV. In a subtle way, *flux* may be increased through lower dispersion, thus concentrating signal in a shorter distance on the detector.

• *The energy resolution* depends on

1) the pinhole aperture
2) the dispersion (drift region length)

The relationship of these user-selected adjustments enable tradeoffs for flux, energy bandwidth, and resolution.

The Design Tool (I)

TPIE was designed to provide exceptional bandwidth and energy resolution for ion energies approaching 1 GeV. Protons, an ion common to all short-pulse laser campaigns, are relativistic at such energies. Accurate modeling of

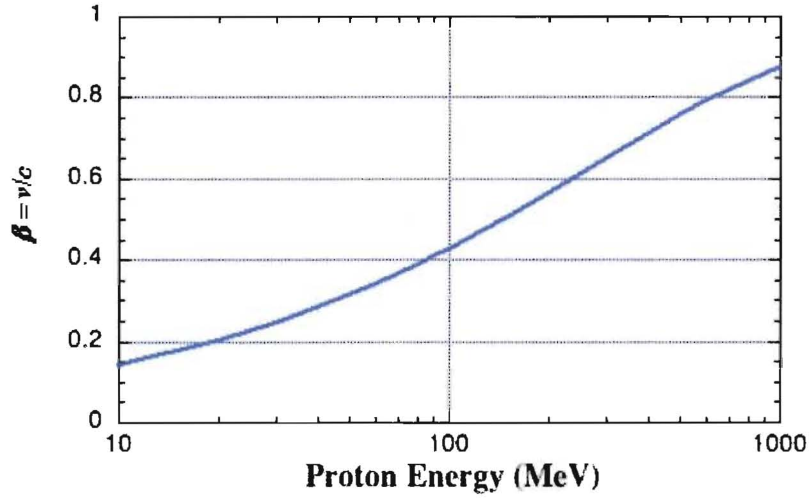

relativistic particle orbits demands a fully relativistic code. Because the relativistic γ and β depend on all velocity components v_x, v_y, v_z, the equations of motion are not separable but are coupled. An iterative solution is necessary. The code was developed using the assumption of constant acceleration for a small time increment δt. It was proven that the solution was stable for $\delta t = 1$ ps, during which time a 100-MeV proton moves < 150 μm. In a field constant over 10 cm, constant acceleration is a good assumption. Code variables are stored in double precision to assure that sufficient decimal places are available for calculations. In the field regions, the accelerations are:

$$\frac{d^2x}{dt^2} = qE / \gamma m_0 \qquad \frac{d^2y}{dt^2} = qBv_z / \gamma m_0 \qquad \frac{d^2z}{dt^2} = -qBv_y / \gamma m_0$$

The Design Tool (II)

The initial conditions for each time step are known or calculated. Then, the usual equations are employed to calculate the new variables (x, y, z, v_x, v_y, v_z, γ) for the next step within the region where the fields are active:

$t(\mathrm{j}) = t(\mathrm{j}-1) + \delta t.$

$$v_\mathrm{i}(\mathrm{j}) = \frac{d^2 x_i}{dt^2}\delta t + v_\mathrm{i}(\mathrm{j}-1).$$

$$x_\mathrm{i}(\mathrm{j}) = x_\mathrm{i}(\mathrm{j}-1) + \tfrac{1}{2}(v_\mathrm{i}(\mathrm{j})^2 - v_\mathrm{i}(\mathrm{j}-1)^2)/\frac{d^2 x_i}{dt^2}.$$

$$\beta(\mathrm{j}) = \sqrt{{v_x}^2 + {v_y}^2 + {v_z}^2}/\mathrm{c}.$$

$$\gamma(\mathrm{j}) = \frac{1}{\sqrt{1-\beta(\mathrm{j})^2}}.$$

One does the bookkeeping for regions where acceleration is zero and then may calculate particle orbits for arbitrary field strengths. With multiple runs of the code, the parameters necessary for design optimization may be found.

Los Alamos
NATIONAL LABORATORY
EST. 1943

Expected Performance

Code predictions for an 80-cm Drift Region, 8 kG, 20 kV/cm: Carbon energy spectrum on CR-39 detector

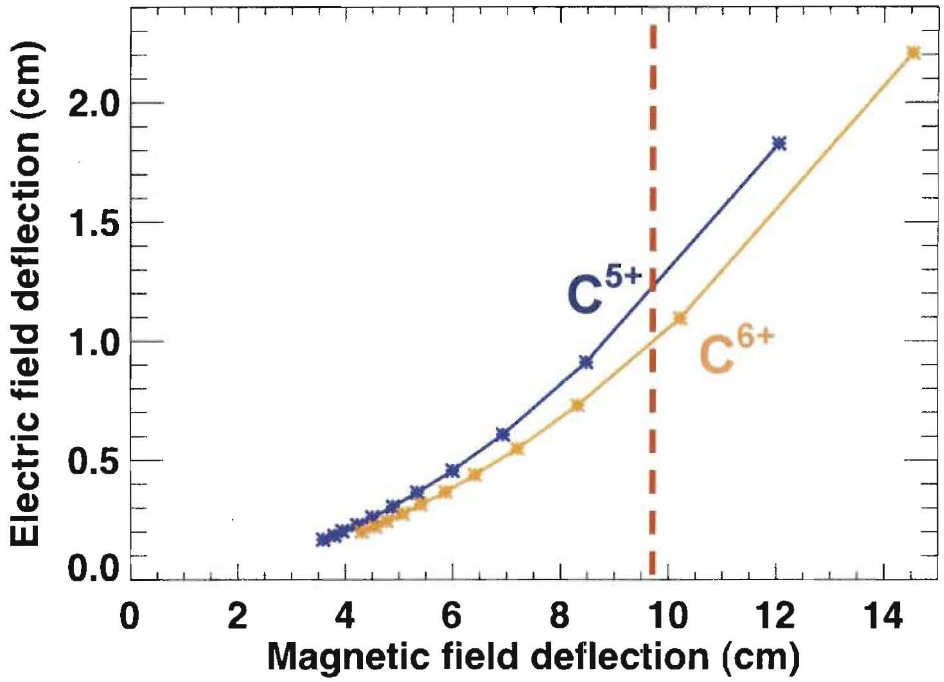

Energies (*) from right-to left: 50, 100, 150, 200, 250, 300,350, 400, 450, 500, 550 MeV

• The ***red line*** is the edge of the standard CR-39. It would see C^{6+} above ~120 MeV, C^{5+} above ~75 MeV. Even with scatter off residual gas, ***TPIE should resolve*** C^{6+} and C^{5+}near 500 MeV. Species separation > pinhole size.

• For lower ion energies, the drift region may be shortened. ***B*** may be changed from 8 kG to 5 kG. Similarly, ***E*** may be adjusted downward: from 20 to 10 kV/cm

• Electrode edge effects are accounted for in the model.

TPIE Geometry

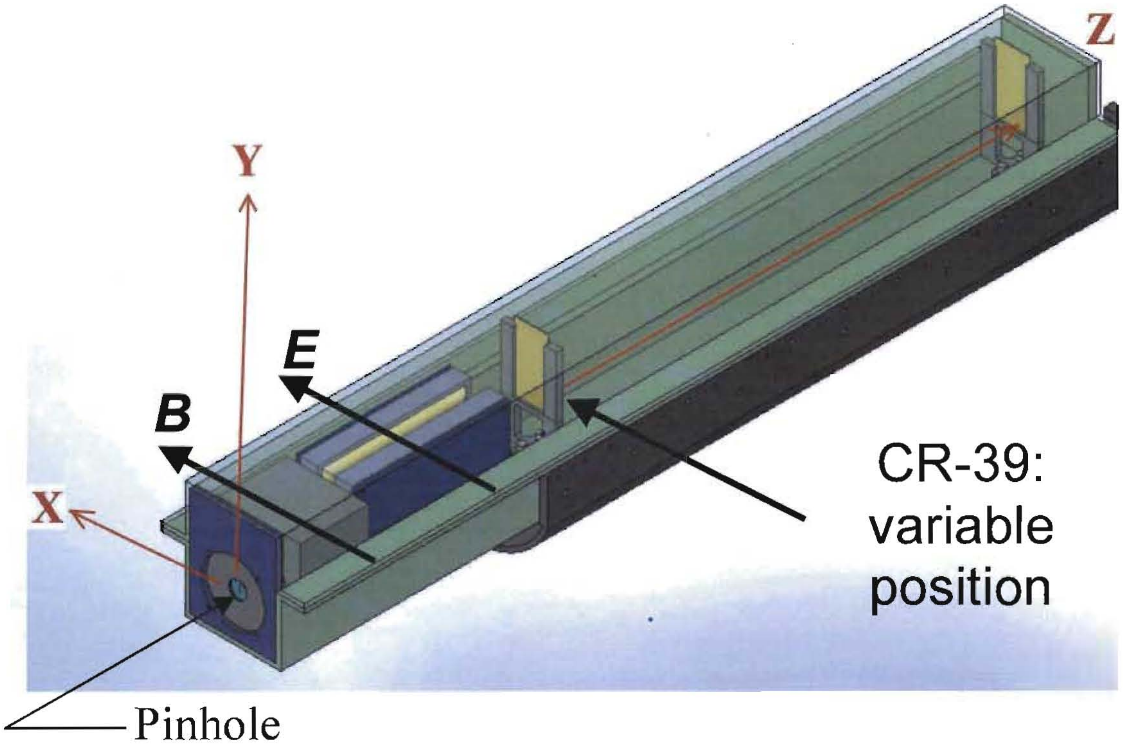

Geometry of TPIE: the magnetic field is at the front behind the pinhole, followed by the parallel electric field region, and two of three detector positions are indicated. The Z axis through the pinhole is the TIM axis.

- $z < 0$: the tungsten nose piece and pinhole
- $z = 0 \rightarrow 10$ cm: the magnetic field
  $z = 0$ is the input plane to the magnet.
- $z = 11 - 31$ cm: the electric field region
- $z = 41$, 81, and 111 cm: this corresponds to detector locations for drift regions of 10, 50, and 80 cm where CR-39 detectors may be positioned
- The detectors are constrained within a goal post.

Tungsten Nose Piece

- 1.6-cm thick W: This thickness corresponds to the stopping distance for ~150 MeV protons.

- Unique design enables 'pinhole dimensions' 100 x 100 µm and 250 x 250 µm.

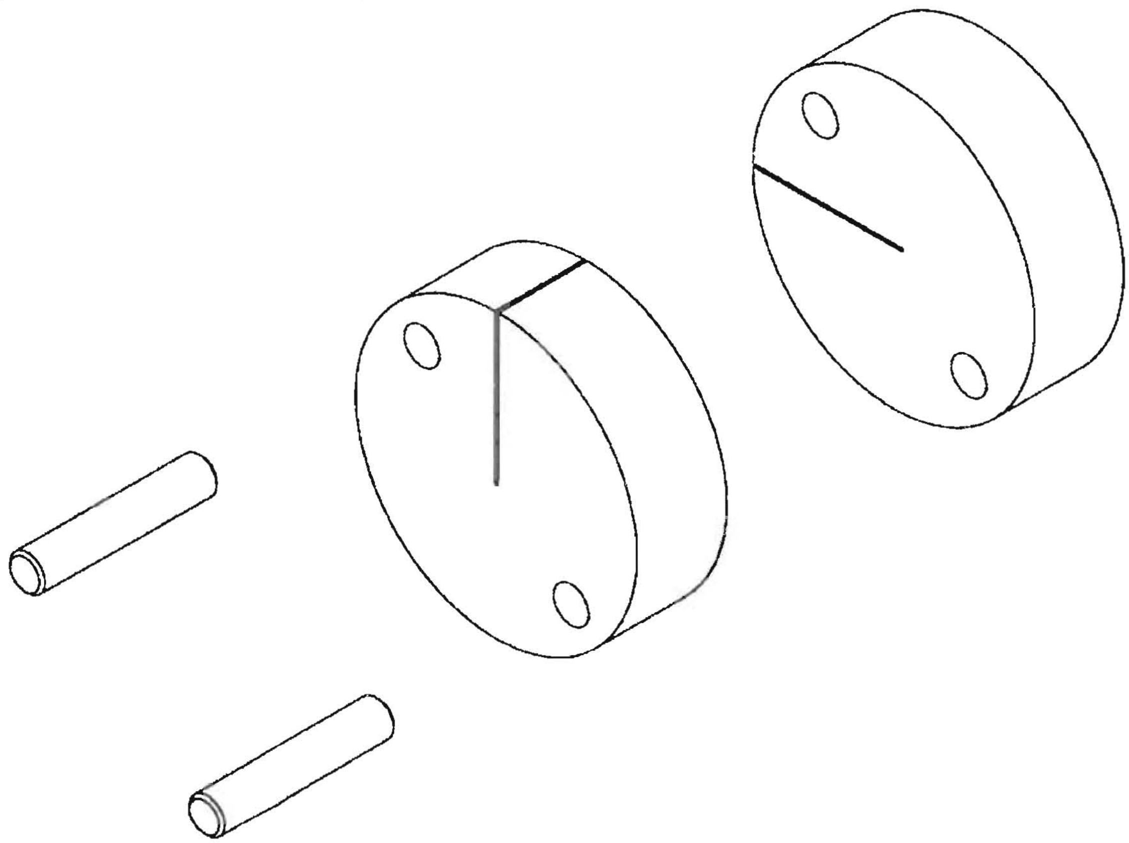

W disks of thickness 0.8-cm are pinned together with W pins. Matching perpendicular slots of width 100 or 250 µm are cut in the two disks, which when joined form a square aperture. The slots are electro-discharge machined. Should higher energy ions be detected, thicker components may be used.

The Magnets

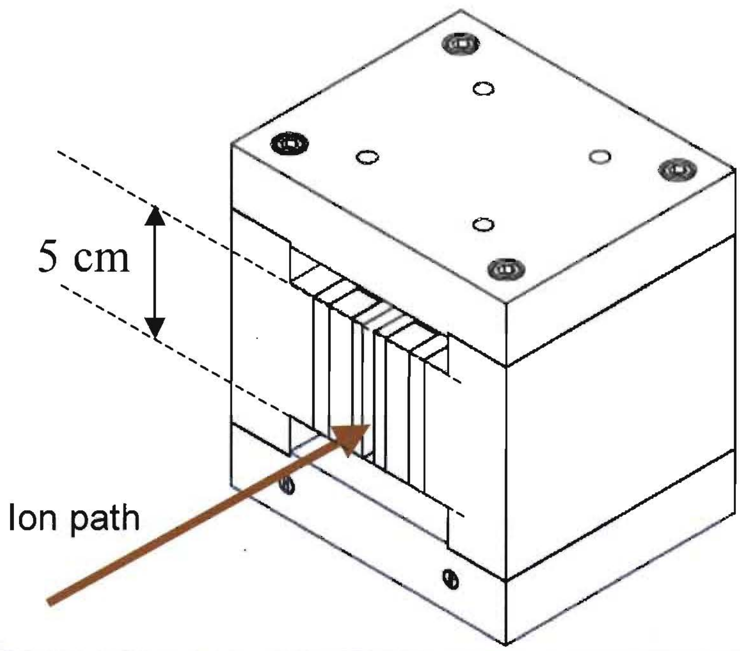

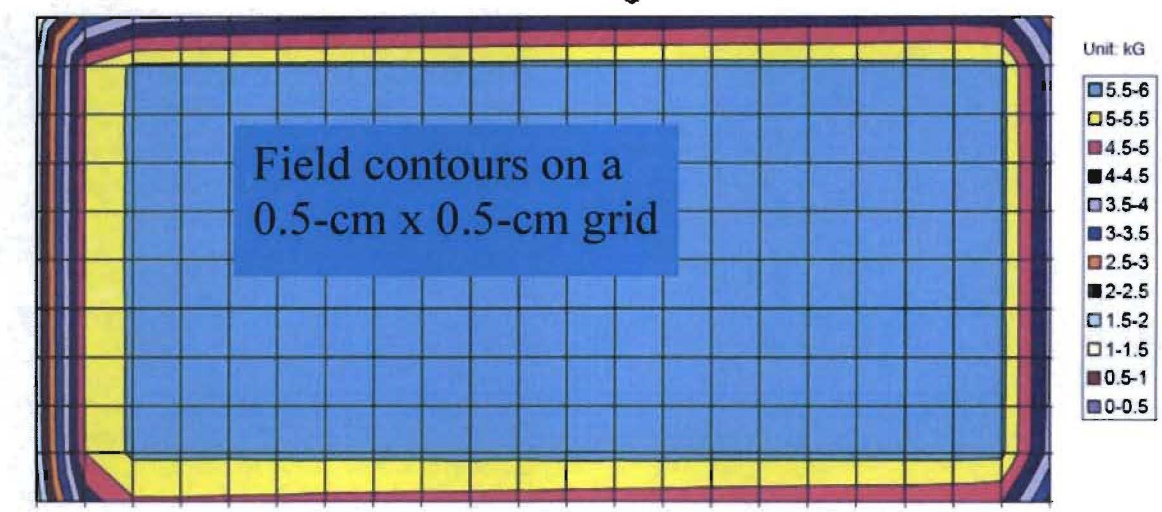

- Length of field region: 10 cm
- Height of field region: 5 cm
- Width of gap: 0.5 cm
- Mean field strength (measured): 5.6 kG ± 5%
- Uniformity: excellent
- Fringing field: minimal
- Because ions drift upward, the *z* axis is below center.

The Electrodes

The goal is to have a uniform electric field between parallel plate electrodes. Experience has shown that ***Rogowski electrodes***, which conform to an equipotential surface, are more benign than semi-infinite plane conductors. See: http://www.nessengr.com/techdata/rogowski/rogowski.html For the latter, the electric field at the edge can be ~7 times the uniform field at interior positions between the electrodes. With Rogowski electrodes, arcing is greatly reduced. Solutions for fringing fields may be calculated.

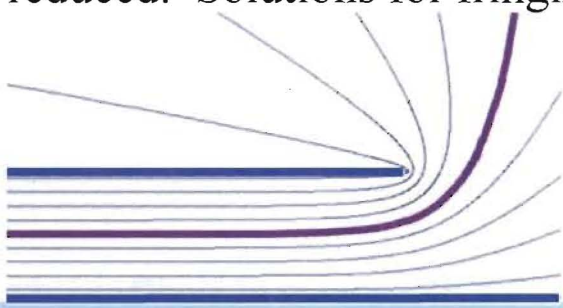

Rogowski profile on TPIE

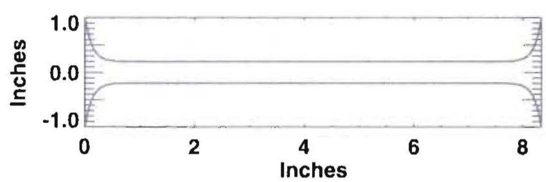

Infinite ground plane below with semi-infinite parallel plane above (both in blue): The violet-colored equipotential corresponds to the chosen shape of Rogowski electrodes for TPIE.

The profile is: $z = a\varphi/\pi$; $x = a/\pi[\pi/2 + e^{\varphi}]$. (I)

- Electrode material: hand polished brass
- Dimensions: 21 x 10 cm^2, 2-cm thick
- Electrode gap: 1 cm
- Housing: KEL-F to protect the edges from arcing
  KEL-F = PolyChloroTriFluoroEthylene (500 V/mil)
- Highest field: ~30 kV/cm
- Electrical connection: from the back through KEL-F

The Fringing Electric Fields

• The region between the ground plane of the magnet and the electrodes is amenable to a conformal mapping solution. One maps:

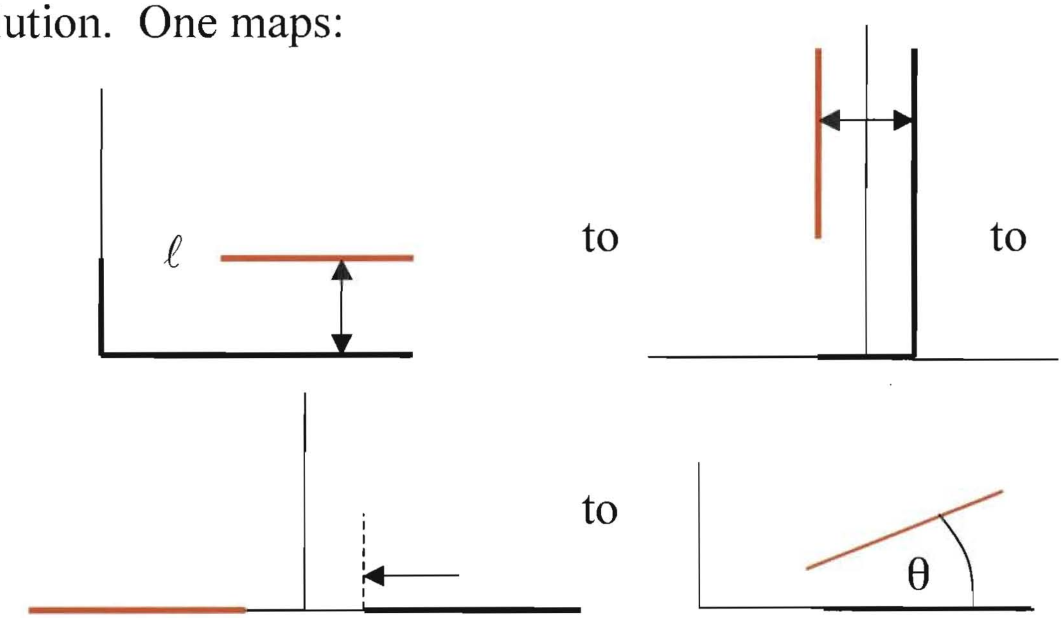

where the red lines represent the high-voltage source and the heavy black is ground. The solution is:

$$\sin \pi x \sinh \pi z = \tan \theta \left(\cos \pi x \cosh \pi z + \tfrac{1}{2}(\cosh \pi \ell + 1)\right)$$

Bounderies: $\ell \geq 0$; $V = V_{max}\, \theta/\pi/2$ where $\pi/2$ corresponds to the Rogowski.

For a given z, x, the voltage may be calculated to good approximation. For a neighboring position, the electric field strength is calculate and applied to the equations of motion. Only the x component is relevant. The z acceleration is completely negligible.

• In similar fashion, the fringing field behind the Rogowski electrodes is calculated from Equ. (I). The equations are transcendental; so the solution is not analytic and is found numerically.

Electrode Control

Electrical power (12 VDC) is introduced to TPIE for the high voltage DC-DC converters by the TIM umbilical cord.

- Pressure interlocked
- Ultravolt 15-A-12-P4(or N4)-C-F-M
- Two separate control circuits: one for each electrode

  Two voltmeters to monitor ± HV

  Two potentiometers to adjust ± HV

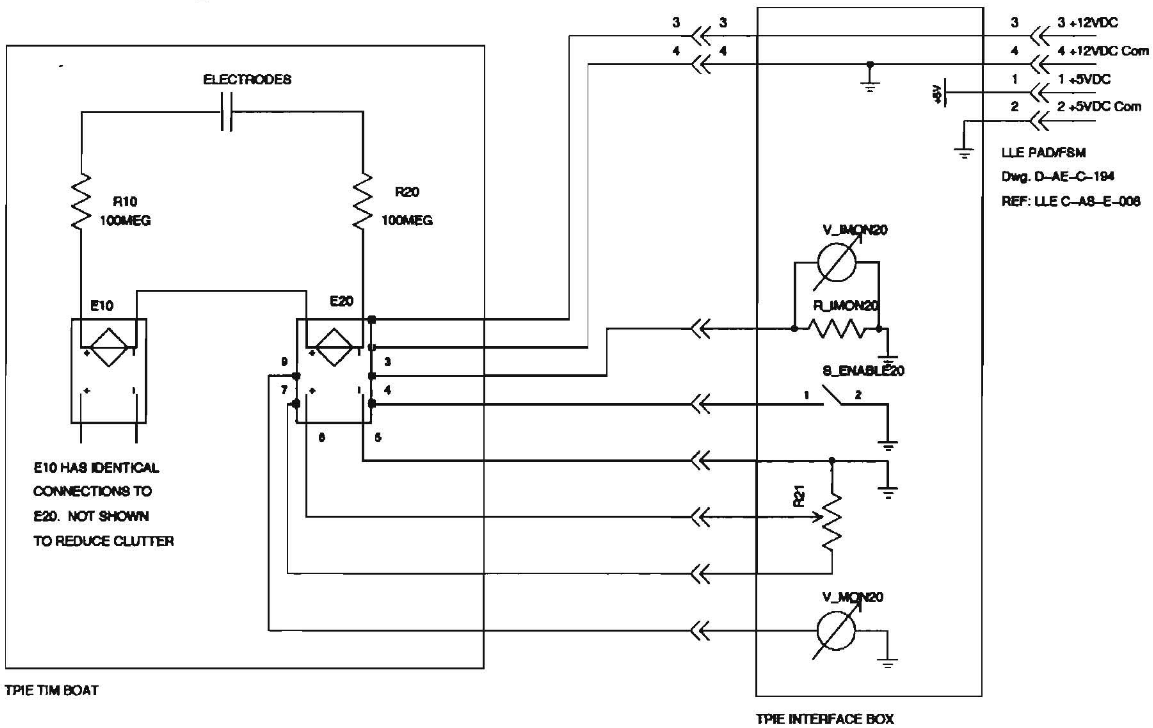

- The pots are linear.
- Positive electrode: DVM = 1.2023 (+HV) – 0.001.
- Negative electrode: DVM = 0.9113 (–HV) – 0.032.

The DVM's are the digital voltmeters. ±HV is the bias voltage on the electrodes. Ions enter the field nearer the positive electrode to reduce scrape off on the negative electrode. The field could be adjusted for ions to enter in the ground plane.

Detectors and Analysis

The user selects one of three detector positions for a drift-region length of 10, 50, or 80 cm. A single sample of 10-cm x 5-cm x 0.1-cm CR-39 is placed at this position. Its stopping power is sufficient to capture protons with energy less than 9.4 MeV. Because many protons are more energetic, we capture them on an image plate behind the CR-39. This means the lowest-energy proton on the image-plate track is ~9.4 MeV. The heavier ions are stopped on the CR-39 also. Both detectors show the 0^{th} order signal from charge-exchange neutrals that travel along the z axis.

For analysis:

- A captured image of 0^{th} order is placed at $x = y = 0$.

- Code results for a selection of ion species and energies are superimposed.

- Possible fit variables are ***magnetic*** and ***electric*** field and ***rotation*** around the 0^{th} order.

- We measure the ***magnetic field*** strength by adjusting it in the code until the start of the proton trace is at 9.4 MeV. [See above.] We then used this value of the magnetic field strength (5.6 kG) in subsequent analysis, and as seen, it is consistent with measurements by the manufacturer.

- Rotation *is not a consideration* for the CR-39 because it is ***constrained*** within the goal posts. The image plate is not precision machined; so the rule for it is not as strict.

- The ***E*** field has been calibrated and is linear.

First TPIE Spectra from EP

This process was used first on ***image-plate*** proton spectra. With very small angular corrections we obtained excellent results:

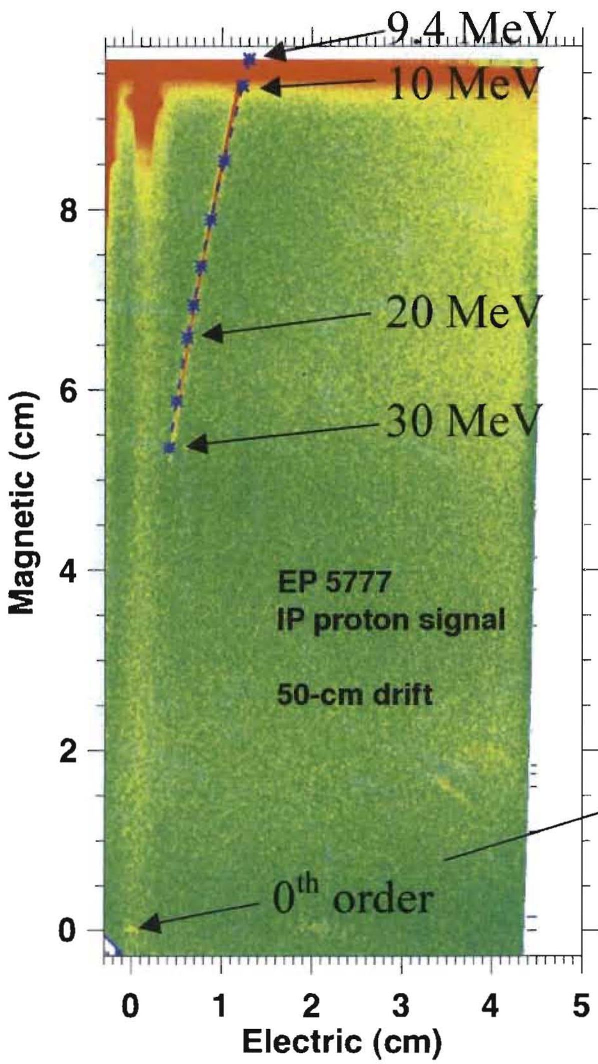

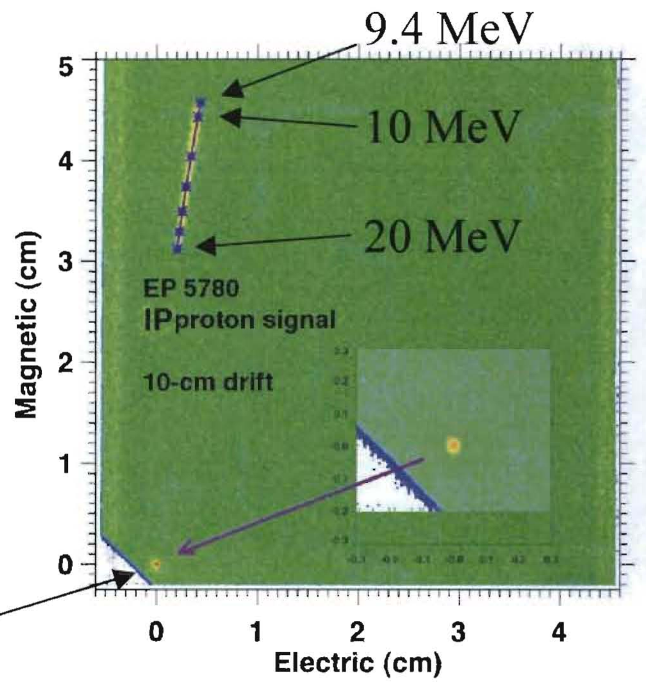

Code results are indicated by blue stars(*).

- Results are consistent with radiochromic film pack data.
- While data were taken near the target normal (highest energy), no attempt was made to optimize EP production of ions. This was a test of TPIE, not of EP.

First CR-39 Data from EP

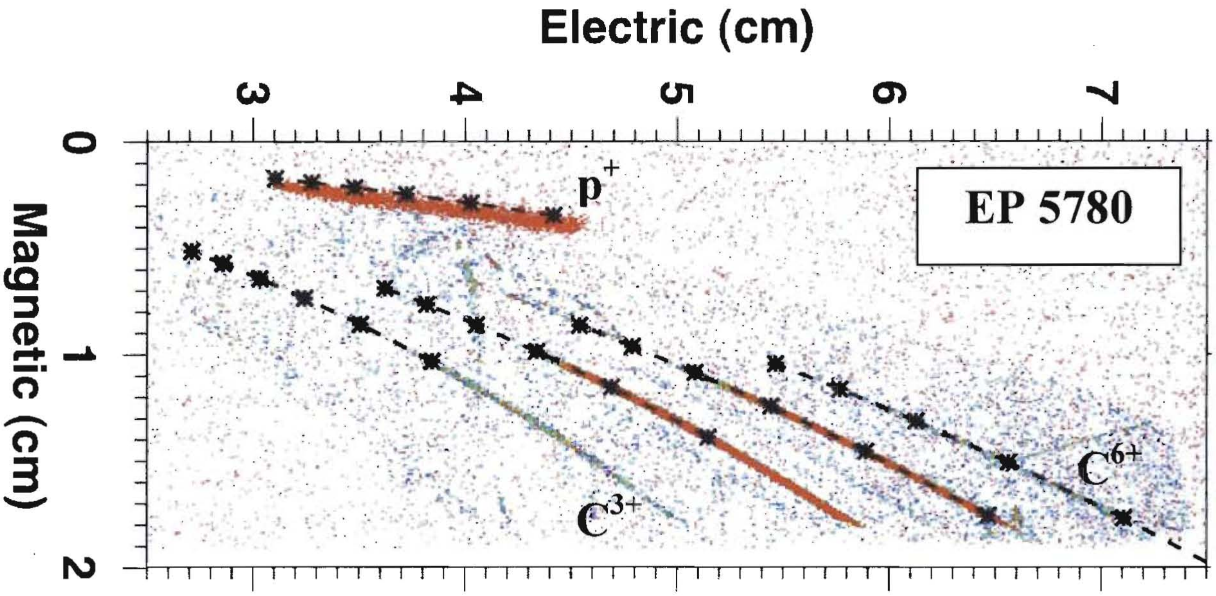

These data are a ***composite of tracks*** from the CR-39 and the IP. The proton trace is from the IP. The C ions are 3+, 4+, 5+, and 6+. There is evidence for O^{5+} and O^{6+}. Beginning from the ***right***, code energy points (*) are ***10, 12, 14, 16, 18, and 20 MeV***.

• To make this fit, the ***electric field*** was reduced from 20 to 17 keV/cm. Our next order of business is to apply the code with the fringing field calculations.

• Max ion energies for this shot: p^{+}~20 MeV, C^{3+} ~10 MeV, C^{4+} ~13 MeV, C^{5+} ~15 MeV, C^{6+} ~18 MeV

• Ion energy spectra will be developed from 'pit-counting' software.

• The C ions are cut off on the low-energy end by impact with the negative electrode.

Signal/Noise and Improvements

Originally, the top of TPIE was uncovered. We found that ions could bounce into the CR-39 without having gone through the W pinhole, resulting in extraneous tracks on the detector.

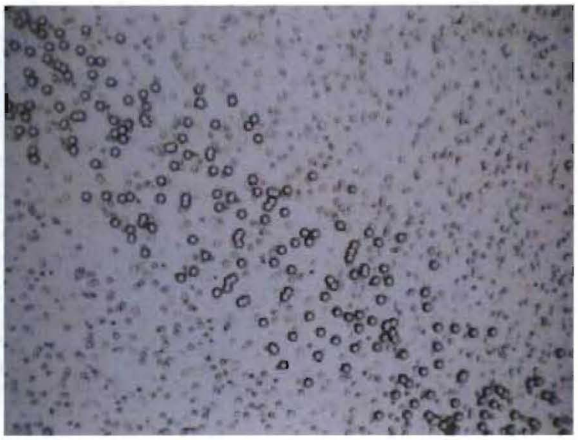

We installed a roof shield over the back end of TPIE to mitigate this problem. The stopping power of the 1/16" Al shroud is sufficient to block the low-energy protons that are the cause.

To the left above, this noise of high-density pits after a 2-hr NaOH etch is pervasive. The larger pits above are due to C ions and have mean diameter ~15 μm. Further etching, while it may erase the noise, will enlarge the C ion tracks so that they merge, and the data become less useful for ion energy spectral analysis.

To the right, we show data taken with the shield in place. Spectral analysis of the ion energy distribution is pending, but we note that the noise is greatly reduced and the ion count rate is substantially higher.

TPIE Summary and Conclusion

- The Thomson parabola for EP performed well during its first use. It is very flexible and has given us a first look at EP ion production.
- It was designed through the use of a fully relativistic ion-orbit code to predict the loci of ion impacts on the detector.
- Versatility is built in to TPIE for flux, dispersion, resolution, and spectral analysis:
  - a) pinhole size
  - b) distance from source
  - c) drift length
- TPIE is TIM-cart compatible, which means that it may be used at other facilities where a TIM is available.
- TPIE is now available for the OMEGA-EP users' community.

Acknowledgements:
Special thanks to Robert Aragonez, Tom Gravlin, Tom Archuleta, Tom Sedillo, and David Clark who have contributed to the development of TPIE and to the OMEGA-EP technical staff who have assisted with its use. Thanks to Michelle Burke and Joe Cowan for assistance with CR-39 etching.

Los Alamos NATIONAL LABORATORY EST. 1943

UNIVERSITY of ROCHESTER